Published in final edited form as:
Neuroimage. 2013 December ; 83: . doi:10.1016/j.neuroimage.2013.07.036.

Neural correlates of time-varying functional connectivity in the rat

Garth John Thompson[a], **Michael Donelyn Merritt**[a], **Wen-Ju Pan**[a], **Matthew Evan Magnuson**[a], **Joshua Koehler Grooms**[a], **Dieter Jaeger**[b], and **Shella Dawn Keilholz**[a,*]

Garth John Thompson: garth@gatech.edu; Michael Donelyn Merritt: mmerritt3@gatech.edu; Wen-Ju Pan: wpan5@emory.edu; Matthew Evan Magnuson: mmagnuson3@gatech.edu; Joshua Koehler Grooms: josh.grooms@gatech.edu; Dieter Jaeger: djaeger@emory.edu; Shella Dawn Keilholz: shella.keilholz@bme.gatech.edu

[a]Georgia Institute of Technology and Emory University, Biomedical Engineering, Atlanta, GA, USA, Postal address: 225 North Ave NW Atlanta, GA 30332, USA

[b]Emory University, Biology, Atlanta, GA, USA, Postal address: 1615 Pierce Dr NE Atlanta, GA 30322, USA

Abstract

Functional connectivity between brain regions, measured with resting state functional magnetic resonance imaging, holds great potential for understanding the basis of behavior and neuropsychiatric diseases. Recently it has become clear that correlations between the blood oxygenation level dependent (BOLD) signals from different areas vary over the course of a typical scan (6–10 minutes in length), though the changes are obscured by standard methods of analysis that assume the relationships are stationary. Unfortunately, because similar variability is observed in signals that share no temporal information, it is unclear which dynamic changes are related to underlying neural events. To examine this question, BOLD data were recorded simultaneously with local field potentials (LFP) from interhemispheric primary somatosensory cortex (SI) in anesthetized rats. LFP signals were converted into band-limited power (BLP) signals including delta, theta, alpha, beta and gamma. Correlation between signals from interhemispheric SI was performed in sliding windows to produce signals of correlation over time for BOLD and each BLP band. Both BOLD and BLP signals showed large changes in correlation over time and the changes in BOLD were significantly correlated to the changes in BLP. The strongest relationship was seen when using the theta, beta and gamma bands. Interestingly, while steady-state BOLD and BLP correlate with the global fMRI signal, dynamic BOLD becomes more like dynamic BLP after the global signal is regressed. As BOLD sliding window connectivity is partially reflecting underlying LFP changes, the present study suggests it may be a valuable method of studying dynamic changes in brain states.

Keywords

functional connectivity; neural basis; sliding window; dynamic; time varying; global signal

*Corresponding author. 101 Woodruff Circle, Suite 2001, Atlanta, GA 30322, USA. Phone number: +1 404-727-2433, Fax: +1 404-727-9873. shella.keilholz@bme.gatech.edu (S.D. Keilholz).

1. Introduction

Resting state functional magnetic resonance imaging (fMRI) has proven a powerful tool for examining regions of the brain that exhibit synchronized activity, referred to as “functional networks” (Biswal et al., 1995; Cordes et al., 2000; Lowe et al., 2000). Originally, networks were assumed to be stationary over the course of an fMRI run (typically six to eight minutes). Early evidence for this assumption came from finding high spatial correlation when comparing two such runs from a given subject (van de Ven et al., 2004) and from finding relationships between functional connectivity and chronic neuropsychiatric disorders (Greicius et al., 2004; Rombouts et al., 2005; Tian et al., 2006; Villalobos et al., 2005).

However, it has become increasingly clear that, while traditional measures of functional connectivity provide an estimate of the ‘average’ relationship between areas, they mask a wealth of information about dynamic interactions within and between networks (Hutchison et al., 2013). Mathematical models of neural-based functional connectivity indicated that if the time scale of connectivity were small enough (30 seconds), variations in functional networks could be observed (Honey et al., 2007). Experimental results from resting state MRI studies have verified this prediction. In rats, Majeed et al. showed that the blood oxygenation level dependent (BOLD) signals exhibit intrinsic spatiotemporal organization, with characteristic patterns persisting for seconds rather than minutes (Majeed et al., 2009). Similar characteristic patterns were subsequently observed using other fMRI contrasts in rats (Magnuson et al., 2010) and using BOLD in humans (Grigg and Grady, 2010; Liu and Duyn, 2013; Majeed et al., 2011). In the diagnosis of schizophrenia, different results were shown for entire fMRI runs versus 96-second long sliding windows (Sakoglu et al., 2010). In healthy individuals, Chang and Glover examined the wavelet coherence and sliding window correlation (120 and 240 second windows) between areas of the default mode network (Fox et al., 2005; Raichle et al., 2001), and found that at certain scales, temporal variability was greater than would be expected by chance (Chang and Glover, 2010). Using sliding window independent component analysis, Kiviniemi et al. showed that the spatial extent of this network varied within individuals (Kiviniemi et al., 2011). This, and other recent studies (Allen et al., 2012; Handwerker et al.; Hutchison et al., 2012) demonstrate that the correlation between areas could vary between strongly positive and strongly negative, features that were not captured by traditional ‘steady-state’ analysis methods. This is not limited to humans, as there have been reports of similar time-varying connectivity in nonhuman primates (Hutchison et al., 2012) and rats (Keilholz et al., 2012).

These findings generated much interest among the neuroimaging community but have been received with a healthy amount of caution due to the difficulty of determining the significance of these variations in connectivity. The spontaneous BOLD fluctuations are low in amplitude and easily contaminated by physiological noise. In addition, the preprocessing that is performed to limit noise contributions adds substantial autocorrelation to the signal. Indeed, two of the studies that reported variations in connectivity found similar dynamics when randomly-matched data were used (Handwerker et al.; Keilholz et al., 2012). Periods of high synchronization across known anatomical connections are a potential sign of the correlation variations having a neural basis; however, in Figure 9 of Hutchison et al. (Hutchison et al., 2012) it is shown that occasional synchronization of the white-matter signal is seen as well, particularly in the shortest (30 second) window. Early evidence that meaningful information can be extracted from dynamic functional connectivity came from Sakoglu et al., who avoided these issues by comparing between schizophrenia patients and healthy controls (Sakoglu et al., 2010). In support of a neural origin for the variability in connectivity, Chang et al. recently presented data from a simultaneous electroencephalography (EEG) and MRI study that suggesting that alpha power is inversely linked to the correlation between the default mode and dorsal attention networks (Chang et

al., 2013). Tagliazucchi et al. reported a similar link between EEG power and functional connectivity using sliding windows (Tagliazucchi et al., 2012). However, while EEG power is typically more directly related to neural activity than fMRI, it is also highly integrative and poorly localized. Patient models, as used by Sakoglu et al., also do not allow direct investigation of the substrate of the functional connectivity changes. Therefore, many gaps are left in our present understanding. An approach is needed that can validate the neural basis of these changes in connectivity.

In the present study, we examine the neural basis of these dynamics by re-analyzing simultaneously recorded electrophysiology and fMRI from the left and right primary somatosensory cortex (SI) of the anesthetized rat using data first reported by Pan et al. (Pan et al., 2011). Our previous work in the rodent identified left and right SI as one of the few pairs of areas where BOLD dynamics were significantly different from those of randomly-matched time courses (Keilholz et al., 2012). By comparing sliding window functional connectivity for the BOLD signal and for band-limited power (BLP), a well-established neural correlate of spontaneous fMRI (Magri et al., 2012; Pan et al., 2011; Shmuel and Leopold, 2008), we show that changes in the correlation of BLP between the left and right electrodes are linked to changes in BOLD correlation, particularly in the higher frequency ranges (25–100Hz) and the theta band (4–8Hz). The correlation between the two increases with the window length used, but longer window lengths increase inter-trial error by more than normalization accounts for and thus may be obscuring the very short dynamics themselves. These findings strongly support a neural origin for at least some portion of the time-varying fMRI connectivity observed in the brain.

2. Materials and Methods

2.1. Animal preparation

All experiments were performed in compliance with NIH guidelines and were approved by the Emory University Institutional Animal Care and Use Committee. The data analyzed were originally acquired for a previous study examining LFP and BOLD correlation for entire fMRI runs using standard analysis techniques, and a more detailed description of experimental procedures can be found in the resulting paper in Brain Connectivity (Pan et al., 2011). Briefly, seven Sprague-Dawley rats (male, 200–300g) were implanted with high impedance (1–5 MΩ) glass microelectrodes in left and right primary somatosensory cortex. A demonstration of the preparation protocol is available in the Journal of Visualized Experiments (Pan et al., 2010). Animals were maintained under anesthesia as they were transferred to the MRI cradle and fixed in the stereotaxic head holder.

2.2. Data acquisition

All imaging was performed on a 9.4 T horizontal bore small animal MRI system (Bruker, Germany). A three plane scout image was first acquired to position the fMRI images. To improve the homogeneity of the magnetic field, the volume of interest (6 mm^3) was shimmed using FASTMAP (Gruetter, 1993). Manual shimming adjustment was applied when necessary to improve the field homogeneity of the selected slice. For fMRI recording, a coronal imaging slice was selected, which included interhemispheric forepaw primary somatosensory areas, in which the glass recording electrodes were implanted. The EPI imaging parameters were FOV, 1.92 × 1.92 cm^2; matrix size, 64 × 64; in-plane resolution, 0.3 × 0.3 mm^2; slice thickness, 2 mm; TR/TE, 500/15 ms. Each fMRI scanning session included 1000 single-slice images acquired over 8.3 minutes. Prior to image collection, twenty unsaved images were acquired prior to each scan to reduce transient signal intensity fluctuations. Resting state runs were collected under concentrations of isoflurane which ranged from 1% – 2%. Isoflurane levels used for specific scans are shown on Table I. The

isoflurane, in a mixture of O_2 and room air, was continuously delivered to the nosecone allowing for free breathing throughout the experiment. The rat's oxygen saturation, measured with a pulse oximeter, was kept above 98% throughout the data acquisition process. One to four simultaneous LFP and fMRI recordings were conducted for each animal. The specific number of scans for each rat is shown on Table I. A total of thirteen runs from seven rats were used. Runs were excluded if they showed head motion spanning more than one voxel total (quantified using Statistical Parametric Mapping, SPM8), if abrupt spike-like head motion was observed, or if noise in electrophysiological data prevented removal of scanner artifacts (see section 2.3).

2.3. Electrophysiology preprocessing

In MATLAB (Mathworks, Natick, MA), artifacts in the raw LFP signal due to the fMRI scanning were removed using a method based on previously established EEG methods (Allen et al., 2000) and described in detail elsewhere (Pan et al., 2010, 2011). To summarize, the saturated portion of the signal that occurs during EPI readout due to rapidly changing gradients (less than 22ms per 500ms) was removed and replaced with a linear function between the two connecting points on each side of the saturation. The non-saturated decaying oscillation that occurs as the amplifier recovers from saturation (approximately 150ms to decay, though the entire 500ms period was used for artifact removal) was removed by averaging across every fMRI run and subtracting the resulting artifact waveform from each to produce a de-noised LFP signal. See Figure 2 in Pan et al. (Pan et al., 2011) for an example.

2.4. Band-limited power calculation

From each LFP signal, six band-limited power (BLP) time courses were created; delta (1–4 Hz), theta (4–8 Hz), alpha (8–14 Hz), low-beta (14–25 Hz), high-beta (25–40 Hz), and gamma (40–100 Hz). The BLP time courses were created by taking the fast Fourier transform (FFT) of de-noised LFP signal segments. Each segment started at the current fMRI image and extended until just prior to the start of the next fMRI image (0.5s per segment, equivalent to one fMRI sample, for alpha and higher frequencies) or extended prior to the start of the third succeeding fMRI image (2s per segment, equivalent to four fMRI samples, for delta and theta). From the FFT of each segment, power values were taken within the frequency band of interest, and these power values had the mean taken in order to create a BLP signal at 2Hz. The resulting BLP signal represents power versus time in each frequency band.

BLP time series were then filtered using a finite impulse response (FIR) filter with a length of 100 seconds to between 0.01 and 0.1Hz, as this frequency range contains statistically significant coherence between BOLD and LFPs in rats anesthetized with isoflurane (Pan et al., 2013). This also matches the range used in previous studies of functional connectivity in isoflurane-anesthetized rats (Liu et al., 2010; Pan et al., 2011).

2.5. fMRI preprocessing

Data analysis was conducted in MATLAB and SPM 8 (http://www.fil.ion.ucl.ac.uk/spm). To summarize, first a brain mask was created, and rows and columns outside the brain were removed from the image. Head motion was corrected using SPM and any runs showing abrupt spikes of head motion or more than one voxel motion were excluded from further analysis. Images were spatially smoothed (Gaussian filter, 0.5 full-width-half-maximum). Linear de-trend was performed on each voxel, setting all voxels to zero mean.

2.6. Global signal regression

Some of the analysis described in this paper was performed with and without global signal regression, in case this correction affected the relationship between BOLD and the electrical activity. Analysis with global signal regression is the default choice due to its common use in similar studies (Liu et al., 2010; Majeed et al., 2009; Pan et al., 2011) and as it removes effects of slight anesthesia differences (Liu et al., 2012). This was done by taking the mean BOLD signal at each time point from all voxels across the brain and regressing this signal from every voxel's individual BOLD signal. Whether global signal was removed or not, all voxel time series were then set to unit variance.

It is worth noting that, when done, the global signal regression was performed only on fMRI derived signals and not on electrophysiological data. LFP and BLP signals are identical between analyses where global signal is or is not removed from functional data.

2.7. Region of interest selection and filtering

As electrodes were implanted only in left and right SI, only these regions were used for further analysis. For each rat, regions of interest (7 to 22 voxels, based on slight differences of the positioning of the slice and the quality of the shim) were manually drawn in left and right primary somatosensory cortex (SI) of the lower forelimb region using an atlas for reference (Paxinos and Watson, 2005). The BOLD signal in each region of interest was averaged across all voxels to produce left and right "SI BOLD signals." These signals were filtered using a filter that matched the one used on BLP time courses (0.01 to 0.1Hz, FIR filter with a length of 100s).

2.8. Normalization of correlation values

The sample Pearson correlation coefficient ("corrcoef" function in *MATLAB*) was used to represent correlation values in this study, r was used to represent individual correlation values and cor(X,Y) used to represent the function of correlation between signals X and Y. As Pearson correlation values are distributed only within [−1, 1], and because correlation of series with fewer points are biased towards higher variance in resulting r values, normalization was performed prior to averaging and prior to statistical tests. This consisted of taking the Fisher transformation (hyperbolic arctangent) of the r values, then dividing the result by one divided by the square root of the number of samples correlated, minus three (the standard deviation of the sampling distribution). This is shown in Equation 1 where **atanh** is the hyperbolic arctangent and **N** is the number of values correlated to produce **r**. This normalization would have created, for hypothetically independent and normally distributed signals, a normal distribution of correlation values (z scores) with a mean of zero and a standard deviation of one.

$$z = \operatorname{atanh}(r) / (1/\sqrt{(N-3)}) \quad \text{Equation 1}$$

2.9. Sliding-window series

Sliding-window correlation was calculated using custom-written software in MATLAB. It was calculated using Pearson correlation, for time windows that were shorter than the entirety of the signals being correlated, incremented by one TR at a time from the beginning of the signals to the end. Adjacent windows overlapped by their length minus one sample. The maximum number of windows was equal to the total number of images, minus the window length, plus one.

For the present study, sliding window correlation was calculated between left and right SI for all BOLD and BLP signals. For comparison to previous studies, Pearson correlation was also calculated over the entire run between the signals from left and right SI for BOLD and for every BLP band. The entire-run *r* values were converted to normalized z values, averaged, and then the inverse transformation was taken to find an estimated average *r* value for comparison to Pan et al. (Pan et al., 2011).

In this report, we will define the term "sliding window series" as the correlation between two interhemispheric signals of the same type (e.g. left SI mean signal from BOLD versus right SI mean signal from BOLD or left gamma BLP versus right gamma BLP, etc.) calculated in a window shorter than the entire signal. The correlation values are ordered and plotted by the time of the window start points. For example, if we state we are correlating the SI BOLD sliding window series with the gamma BLP sliding window series, we are generating a time-ordered series of correlation values for left SI BOLD versus right SI BOLD, then generating a time-ordered series of correlation values for left gamma BLP versus right gamma BLP. Subsequently, because each of these individual sliding window series is itself a time course of correlation data, they can then be correlated themselves to produce a single correlation value between two different sliding window series, e.g. cor(SI BOLD sliding window series, gamma BLP sliding window series).

2.10. BLP sliding window series correlated with BOLD sliding window series

The sliding window series from interhemispheric SI BOLD was compared to each sliding window series from interhemispheric BLP by computing Pearson correlation between the corresponding BLP and SI BOLD sliding window series for every run, e.g. cor(SI BOLD sliding window series, gamma BLP sliding window series), etc. This was computed separately for each frequency band of BLP, so that each band could be examined individually.

As we expected the BOLD sliding window series to follow the BLP sliding window series due to the hemodynamic delay, BLP sliding window series were delayed four seconds relative to SI BOLD sliding window series to match when peak correlation was observed in steady-state findings (Pan et al., 2011). Preliminary work was done to see if a peak correlation based on time shift could be found for BLP sliding window series being correlated with SI BOLD sliding window series; however, due to the small sample size the standard error was too large to make inferences (allowing shifts up to ±100s, standard error in optimal time shift rounded to 6s ± 7.5s for theta, high beta and gamma, and −5s ± 9.5s for delta, alpha and low beta, mean ± standard error).

For this analysis, a 50s window length was selected to match previous work with fMRI-only data (Keilholz et al., 2012). (For further justification, see section 4.3 in the discussion.) All *r* values were normalized to z values and the mean z value was then taken across all rats, runs and time points for both SI BOLD and every BLP.

2.11. Dependence on window length

To investigate effects of window length on results, the calculation of sliding window series was repeated for window lengths of 10 to 100 seconds (the filter's pass-band) in 0.5 second increments. First, all *r* values were converted to normalized z values and the mean z value was then taken across all rats, runs and time points for SI BOLD and every BLP signal as a function of window length. Second, for every fMRI run, window length and BLP band, Pearson correlation was calculated between every run's sliding window series from SI BOLD and that run's sliding window series from each BLP band, shifted 4s prior, e.g. cor(SI BOLD sliding window series with 10s windows, gamma BLP sliding window series

with 10s windows) to cor(SI BOLD sliding window series with 100s windows, gamma BLP sliding window series with 100s windows), etc. Resulting *r* values were converted to normalized z values. Both of these tests were repeated without normalization on naïve *r* values.

2.12. Correlation with global signal

As regression of the global signal from every voxel in BOLD was found to increase correlation between BOLD sliding window series and BLP sliding window series (see section 3.2), it is possible that the global signal acts as a confounding factor to sliding window analysis. This is surprising as it contradicts previous studies that have indicated the global signal reflects underlying neural activity (Scholvinck et al., 2010). However, the "global signal" measured here is likely the result of several factors which are difficult to disentangle, including global neural modulation, common physiological noise, (Fox et al., 2009) and contributions from large networks as only a single slice was imaged (Majeed et al., 2009; Williams et al., 2010). Therefore, a further investigation of the effects of the global signal was performed. The global signals (calculated from the mean fMRI signal from all brain voxels) were saved from every run during section 2.6. Prior to the analysis done in section 2.12, a linear de-trend was performed on these global signals, they were then set to unit variance and filtered to the same pass-band as the other signals analyzed in this study (0.01 to 0.1Hz, FIR filter with a length of 100s).

Standard Pearson correlation coefficients were calculated for each global signal versus either the corresponding BLP signal (six bands) or the corresponding SI BOLD signal. Correlation between the global signal and SI BOLD was calculated without global regression performed on the SI BOLD data. In every case where it was compared to a BOLD-derived signal (SI BOLD or the global signal), the BLP signal was lagged by four seconds. These coefficients (*r* values) were converted to normalized z values as was described in section 2.8. Data from each of the two hemispheres were combined for statistical analysis.

In addition to direct relationships between measured neurophysiological signals and the global signal, it is also possible that increases/decreases in the global signal increase/decrease correlation across the entire brain. This is because a strong global signal, even one arising from a neural source, could obscure local variations in correlation by increasing correlation across the entire brain. In particular, it is possible that changes over time in the BLP sliding window series may be driven by the magnitude of the global signal if the global signal is driving network dynamics (Scholvinck et al., 2010). To investigate this, the sliding window series (interhemispheric correlation calculated in 50s sliding windows for the corresponding signal) for SI BOLD and for each BLP band was also correlated with the global signal using standard Pearson correlation. Note that SI BOLD was used both with and without global regression here because global regression was done only on BOLD amplitudes on a per voxel basis, not considering correlations between voxels, and thus the sliding window series from SI BOLD with global regression performed had the possibility to remain highly correlated with the global signal. All correlations between sliding window series (from BOLD or BLP) and the global signal (from BOLD) were done at multiple alignments; these alignments corresponded to every possible alignment between a point in the global signal and where that point was located within the corresponding window (−25s to 25s, relative to center of window). In addition, in every case where it was compared to a BLP-derived sliding window series, the global signal was moved backward in time by four seconds. These coefficients (*r* values) were converted to normalized z values as was described in section 2.8.

To examine the relationship between BLP, SI BOLD and the global signal in the steady-state, a full partial correlation analysis was done on signals from entire runs ("partialcorr"

function in *MATLAB*). This compared every set of two of these signals for correlation and the third signal was considered to be a controlling variable. As all BLP data for a given run are generated from the same LFP data trace, each frequency band was considered separately for the partial correlation analysis to avoid biasing results. As partial correlation uses linear regression, only the BOLD signals without global signal regression were used for this analysis. The SI BOLD and global signals were moved back in time by four seconds relative to the BLP. Only entire runs were examined for this analysis; due to not finding significance in prior analysis (Supplemental Figure S4), no sliding window series were examined, only the original SI BOLD and BLP signals. Data from each of the two hemispheres were combined for statistical analysis.

2.13. Determination of significance

To minimize the chance that correlation observed between the two sliding window series was due to inherent characteristics of the processed signal, artificial null distributions were created for comparison. The correlation between BOLD and BLP sliding window series' time courses for the artificial null distribution was calculated in the same manner as for the real data, but each BLP signal was paired with a BOLD signal from a different fMRI run. For correlation with the global signal, the same process was done except the BLP, BOLD or sliding window series signals were paired with global signals from different fMRI runs. In each case, every trial was compared to every trial with an index number higher than its own index, to create a large null distribution from the upper triangular half of the comparisons matrix ($[13^2-13]/2 = 78$ total incorrect comparisons). When three series (BLP, SI BOLD and global signal) were compared during partial correlation analysis, all three series were mismatched by taking every SI BOLD trial with a higher index number than the BLP, and taking the global signals with every index number different than both the BLP index number and the BOLD index number. (These particular incorrect pairings were chosen as they were the most basic to implement in *MATLAB* and resulted in 936 total incorrect comparisons.) For each comparison, a two sample, two-tailed, equal variance student's t test was calculated between the distribution of actual z scores and the null distribution of z scores. To correct against false positive errors due to multiple comparisons, sequential goodness of fit (SGoF) (Carvajal-Rodriguez et al., 2009), a binomial-based method of controlling family-wise error rate (FWER), was calculated to determine a threshold for significance with a 5% FWER. Each figure or table was considered one family for statistical purposes.

3. Results

3.1. Sliding-window correlation

Both BOLD and BLP correlation time courses calculated with a sliding window approach ("sliding window series") exhibited interesting variability in all rats. An example from one rat (first run, index = 1 from Table I) is shown in Figure 1. This rat is typical as its gamma and beta bands have mostly positive values. The changes in correlation over time are not limited to the BOLD signal but also can be observed in the BLP signals, which implies that a neural origin is possible for the variation in connectivity measured with BOLD.

"Steady-state" correlation was calculated for each time course using data from the full run for BOLD and for each BLP band. The results are given in Table II as both actual mean z values and estimated r value averages that are in close agreement with previous analysis of this data presented in Figure 7 of Pan et al. (Pan et al., 2011). Correlation between BLP from left and right SI is highest for beta and gamma bands and lowest for delta and theta bands.

3.2. BLP sliding window series correlated with BOLD sliding window series

To examine the relationship between variations in BOLD correlation and in BLP correlation, the sliding window series from each BLP band was correlated with the SI BOLD sliding window series from the same fMRI run with BLP lagged by four seconds to match Pan et al. (Pan et al., 2011). 50s windows were used for this analysis. Note that four seconds may not be an exact match, as delta and theta used 2s power spectrum windows instead of 0.5s power spectrum windows for power calculations, causing each window in the SI BOLD sliding window series to potentially align with up to four windows in the delta and theta BLP sliding window series. As a control, correlation was also calculated by mismatching which SI BOLD sliding window series went with which BLP sliding window series, destroying common temporal information.

The results are shown in Figure 2. After SGoF correction for multiple comparisons, theta, high beta and gamma sliding window series were significantly correlated with the SI BOLD time courses ($p=1.35\times10^{-3}$, 8.40×10^{-6} and 5.18×10^{-5} respectively). The strongest correlations were observed in the high beta and gamma frequencies. As the use of global signal regression has been debated (Fox et al., 2009; Gavrilescu et al., 2002), the same calculation was also performed without the use of global signal regression as a preprocessing step. Correlation in all frequency bands was lower when global regression was not used; however, results were similar. The decrease was greater in the statistically significant frequency bands (mean $\Delta z = 1.67$ for statistically significant bands, mean $\Delta z = 0.872$ for non-statistically significant bands). Theta, high beta and gamma again passed correction for multiple comparisons when no global signal regression was used ($p=7.20\times10^{-3}$, 1.35×10^{-3} and 1.81×10^{-3} respectively).

3.3. Dependence on window length

Correlation was also calculated between interhemispheric SI signals to create sliding window series using a large range of window lengths for both SI BOLD and BLP. Positive correlation was observed in all frequency bands even for the shortest windows, and the correlation increased with window length for the entire filter pass-band from 10s to 100s (Figure 3). This monotonic increase may be partially due to normalization of *r* values to z values; longer windows correlate more samples and thus normalization increases correlation values (Supplemental figure S1a). Naïve correlation values also showed an increase in correlation with window length, but a plateau was reached at approximately 50s (Supplemental figure S1b).

Numerical values at window lengths of 10s, 50s and 100s are shown in Table III for comparison for both normalized and naïve correlation values. For normalized correlation values, at 50s every BLP band had reached only approximately 40% of the maximum value reached over all window lengths (Delta, 38%, Theta, 35%, Alpha, 36%, Low beta, 38%, High beta, 39%, Gamma, 39%) and SI BOLD had reached 67% of the maximum value over all window lengths. For naïve correlation values, at 50s every BLP band had reached approximately 90% of the maximum value reached over all window lengths (Delta, 87%, Theta, 87%, Alpha, 90%, Low beta, 94%, High beta, 92%, Gamma, 92%) and SI BOLD had reached 91% of the maximum value over all window lengths.

Correlation was also calculated, for every window length and BLP band, between SI BOLD sliding window series and all BLP sliding window series, with BLP time shifted four seconds prior to SI BOLD. Results are shown in Figure 4. Mean Z values for all bands are plotted versus window length in (A) and standard error of Z values are plotted versus window length in (B). From 10s to 18s window lengths all bands show increasing correlation with increasing window length, and all bands also show positive mean

correlation with window lengths within the entire pass-band. Delta and low beta first peak (first switch from increasing to decreasing) at relatively low lengths (18.5s and 29.5s window lengths respectively), high beta, gamma, and alpha peak later, in that order (67.5s, 68s and 71.5s window lengths respectively). Naïve correlation values, shown in Supplemental figure S2, show an almost identical trend.

Figure 4B illustrates the corresponding standard error values, also plotted in Figure 4A as error bars. Error increases rapidly for all bands for the entire pass-band. This is seen even though normalization biased error towards lower values for longer window lengths, as shown in Supplemental figure S2A.

3.4. Correlation with global signal

Standard Pearson correlation was calculated between each SI BOLD and BLP signal (six frequency bands) and the corresponding global signal. Significance was tested by comparing versus data where the global signals had been mismatched (see section 2.13). These results are shown in Supplemental Figure S3; strong significant correlation was shown between the SI BOLD signal (without the global signal regressed) and the global signal itself, weaker significant correlation was shown between theta and higher frequency BLP bands and the global signal. This result matched previous observations of correlations between electrophysiology and global BOLD (Scholvinck et al., 2010).

Standard Pearson correlation was also calculated between sliding window series calculated from 50s windows and the global signal. This was done for multiple alignments between the sliding window series and the global signal, ranging from each point in the sliding window series aligned to the equivalent of the start of its window in the global signal to the equivalent of the end of its window in the global signal.

Significance was tested by comparing versus data where the global signals had been mismatched (see section 2.13). When BOLD with the global signal regressed or BLP signals were used to calculate the sliding window series, there was no statistically significant relationship between the sliding window series and the global signal (no p values less than 0.05 with or without correction for multiple comparisons, see Supplemental Figure S4 for a histogram of p values). However, when BOLD without the global signal regressed was used to calculate the sliding window series, a significant relationship was seen at offsets from 17.5s to 25s (aligning the global signal relative to the right of center of the sliding window). These values were negative and ranged from z values of −2.52 to −3.03. This result is shown in Figure 5 as a plot of z value (for correlation between global signal and SI BOLD sliding window series). This result suggests that as global signal increases, measurement of sliding window correlation in BOLD decreases, and/or vice-versa.

For each BLP frequency band separately, a partial correlation analysis was done between SI BOLD (without global signal regression), BLP from the corresponding electrode and the global signal. This analysis calculated correlation between each pair of signals while considering the third signal to be a controlling variable. Significance was tested by comparing versus data where all three signals had been mismatched (see section 2.13). The results are shown in Table IV. A statistically significant difference from incorrectly matched data was seen in theta, beta and gamma BLP bands in terms of their relationship with SI BOLD. The reason alpha is not statistically significant despite having a slightly higher z score than theta is because it had slightly higher errors in both correctly and incorrectly matched data. No matter which BLP band was included as a controlling variable, SI BOLD and the global signal were still significantly correlated. However, when SI BOLD was used as a controlling variable, no BLP band showed a significant relationship with the global signal.

In constructing Table IV, very low p values were observed for many "non-significant" cases. If standard Bonferroni FWER correction was used instead of SGoF, the threshold for significance was $p \leq 2.8\times10^{-3}$ instead of $p \leq 1.70\times10^{-31}$. In this case, all partial correlations between BLP and SI BOLD and all partial correlations between SI BOLD and global BOLD are significant. BLP and global BOLD are significantly partially correlated only for the delta band, all other BLP bands remain non-significant.

The results from partial correlation analysis (Table IV) would suggest that the correlations between BLP and the global signal (Supplemental figure S3) are due to their relationship with local BOLD and local BOLD either influencing or being influenced by the global signal, not due to directly influencing or directly being influenced by the global signal itself.

4. Discussion

This study provides the first evidence that the time-varying connectivity observed with resting state MRI (Chang and Glover, 2010; Hutchison et al., 2012; Keilholz et al., 2012) reflects changes in correlation of neural field potentials observed directly from the brain. The gamma, high beta and theta bands show a significant relationship between changes in LFP power correlation and changes in BOLD correlation (Figure 2). The finding of a neural basis for at least some of the variability in BOLD correlation is important, as previous studies demonstrated that similar variations could arise from randomly-matched or modeled time courses (Handwerker et al., 2012; Keilholz et al., 2012). These findings also agree with data showing that variations in network connectivity on short time scales can predict task performance such as vigilance (Thompson et al., 2012) and diseases such as schizophrenia (Sakoglu et al., 2010).

4.1. Comparison to previous analysis

The analysis performed in this study utilized data acquired in order to compare steady-state functional connectivity to coherent neural activity as a function of anesthesia level (Pan et al., 2011). Pan et al. observed high frequency BLP was most correlated across hemispheres and also contributed the most to the local BOLD signal, although all frequency bands were strongly correlated with BOLD at a lag time of 4s. However, only delta and theta correlation were predictive of BOLD correlation as the level of anesthesia varied, in agreement with the previous study by Liu et al. (Liu et al., 2010). Anesthetic depth was not investigated in the present study, as data were pooled to provide greater statistical power. As the variation between frequency bands was clear regardless of variation in anesthetic levels (Figure 7 in Pan, et al. (Pan et al., 2011)) the slight differences in anesthetic levels should not invalidate the present study.

The link between correlation in the delta and theta bands and BOLD, observed in the study by Pan et al., may have been caused by effects of anesthesia depth other than the overall reduction in neural correlation. The mechanism of neural suppression in isoflurane is likely inhibition of thalamocortical GABA and glutamate receptors (Alkire et al., 2000), while the mechanism of vascular dilation may be separate and due to blockage of adenoside-triphosphate sensitive potassium channels (Cason et al., 1994). Both of these effects would increase with anesthetic depth. The present study showed a significant BOLD-BLP relationship for high beta and gamma bands, but not for delta, and theta remained significant (Figure 2). This may indicate that differing levels of neural suppression are behind the relationship between delta and BOLD seen in Pan, et al., Figure 9, rather than an implied delta-BOLD coordination.

4.2 Comparison to other animal and human studies

In the present study, the higher frequency BLPs were most closely related to BOLD changes. The comparatively high correlation values in these frequency bands are in close agreement with results linking BOLD fluctuations to LFPs recorded from a single site in nonhuman primates under different anesthetics (Magri et al., 2012; Shmuel and Leopold, 2008). This suggests the present results are not restricted to isoflurane and supports the idea that at least some of the BOLD fluctuations reflect variations in local activity linked to high frequency LFPs. The only other band that was statistically significant was theta (Figure 2). This is interesting as theta's phase may be coupled to amplitudes of higher frequency activity such as gamma (Canolty and Knight, 2010; Tort et al., 2010) which also may be coupled to amplitudes of infraslow oscillations (0.01 to 1Hz) measured with EEG (Monto et al., 2008). The present study measured infraslow BOLD fluctuations, which are standard in functional connectivity, but did not use electrical amplifiers that could record LFP in this range. However, the infraslow LFP may also contain interesting dynamic correlations; Pan et al. recently showed that the BOLD signal is tightly coupled to very slow electrical oscillations (<1 Hz) (Pan et al., 2013). It is widely hypothesized in neuroscience that low frequency electrical activity organizes and coordinates large areas of the brain, while high frequency activity coordinates local interactions (Canolty and Knight, 2010). If this is true, the spontaneous BOLD fluctuations may reflect a combination of large scale patterns of quasi-periodic (displaying periodicity, but irregularly) modulation of excitability and localized fluctuations linked to local processing. It may then be possible to separate the large scale, quasi-periodic patterns from more variable changes in local activity (Majeed et al., 2011; Majeed et al., 2009), extracting new information about the neural organization of the brain. The sliding window approach used in this study may be weighted toward these local variations. Future work including the very low frequencies will help to elucidate the sources of the variation.

In humans, Chang et al. found a relationship between alpha power in the EEG and connectivity between two networks, the default mode and dorsal attention networks (Chang et al., 2013). Tagliazucchi et al. observed that increased power in the alpha and beta bands was associated with decreases in functional connectivity, while increased gamma power was linked to increased functional connectivity (Tagliazucchi et al., 2012). It should also be noted that while the studies by Chang et al. and Tagliazucchi et al. examined the relationship between connectivity and EEG power, our study focused on the correlation between BLP from areas in the left and right hemispheres as compared to the correlation between the BOLD signals from the same areas. The frequency distribution of EEG power is related to the level of the subject's alertness, and therefore it is possible that the relationship between alpha power, for example, and BOLD is a result of fluctuations in the subject's drowsiness level. This is supported by the study by Tagliazucchi et al, which found that the relationship between EEG power and BOLD was altered in subjects with changing levels of alertness. Because the rats in our study were anesthetized and electrical signals were obtained using intracortical recordings that provide better spatial localization, our findings strengthen the evidence that the changes in correlation seen in human studies are linked to changes in local neural coordination, rather than only large-scale behavioral states.

4.3. Window length dependence

BOLD and all BLP exhibited lower interhemispheric correlation when shorter windows were used. This may have been partially due to the normalization of z scores favoring longer window lengths which correlated more values (Supplemental figure S1A), because naïve correlation values also increased, but reached a plateau around 50s (Supplemental figure S1B). Based on Sakoglu et al. (Sakoglu et al., 2010), a minimally sufficient window length can be selected as 0.5 divided by the minimum frequency in the signal. In the present study

it was 0.5 / 0.01Hz = 50 seconds. In addition, a recent report by Allen et al., found that window lengths between 30 and 120 s had little impact on the resulting dynamics (Allen et al., 2012). In the present study, however, a 50s window length was able to capture only 67% of maximum BOLD interhemispheric correlation when normalized to z values, but this increased to 91% when naïve *r* values were used. This suggests that longer window length provides greater confidence in results (represented by normalization increasing values more), even if raw *r* values do not increase greatly after the minimum suggested by Sakoglu et al.

The results from correlating BOLD and BLP sliding window series (Figure 4) suggest that choice of window length may reflect a trade-off between shorter window lengths, which produce lower correlation but lower error, and longer window lengths, which increase correlation as they increase error. Note that this increase in error occurred in opposition to normalization which decreased z scores and thus was more likely to decrease error as window length increased (Supplemental figure S2). This result suggests that shorter windows may, in fact, reflect transient neural events which are synchronized between BOLD and electrophysiology. These result in low inter-trial error but, due to their transient nature, have low signal to noise ratio and thus low correlation. However longer windows may reflect a general BOLD-BLP relationship that can have very high correlation due to averaging over long periods, but may be occluded by transient events in some runs, leading to high inter-trial error.

Combining these factors, a smaller window length is advantageous due to its ability to more accurately represent transient events that may be merged over longer windows, and due to a lower inter-trial variability when BOLD is compared to electrophysiology. A longer window length increases the signal to noise ratio and provides more confidence in correlation results, and thus can be used in situations where differences between groups are more subtle. This confirms what has been seen in previous studies, as the shortest window length permitted by the filter's pass-band was effective in diagnosing network differences a few seconds before a task was performed (Thompson et al., 2012), while a window length slightly longer than the filter's pass-band was effective in diagnosing schizophrenia over entire resting-state scans (Sakoglu et al., 2010).

4.4. Effects of global signal regression

In the present study, correlation was observed between the global signal from whole-brain BOLD and several BLP bands, replicating results previously seen by Scholvinck et al. (Scholvinck et al., 2010). Seen alone, such findings might suggest a neural electrical source for the relevant part of the global signal. It would then follow that changes in correlation over time between two brain regions are due to increasing or decreasing global signal obscuring the inherent local correlation of a network. However, further investigation showed this was not true as the global signal did not positively correlate with any BLP sliding window series and negatively correlated with SI BOLD only if no regression was performed (Figure 5, Supplemental Figure S4). In addition, partial correlation (Table IV) suggested that the correlation between the global signal and BLP was due to the strong relationship between BLP and SI BOLD, and between SI BOLD and the global signal, rather than a direct relationship between the global signal and BLP. Supporting this result was the observation (Figure 2) that regression of the global signal results in a stronger correlation between SI BOLD sliding window series and BLP sliding window series. In other words, the functional connectivity between interhemispheric SI measured with BOLD better represents the functional connectivity measured with BLP if the global signal has been regressed. Altogether, these results would suggest that, when performing sliding window analysis of functional connectivity, the global signal may be a confounding factor rather than representing connectivity in the underlying neural activity.

However, these results must be viewed with caution for several reasons. First, the global signal is not monolithic and may represent both global neural modulation and non-neural physiological noise (Fox et al., 2009). Second, the results are affected by the nature of the animal model used. The rats were imaged under isoflurane anesthesia which is a potent vasodilator (Cason et al., 1994; Reiz et al., 1983) and only a single coronal slice of the brain was imaged. Under increasing concentrations of isoflurane the global signal becomes increasingly strong (Liu et al., 2012) and therefore may not represent the same physiological mechanism that is observed in awake humans. As the single slice that was imaged was mostly composed of the cortex and the caudate-putamen, and as the cortex and caudate-putamen are functionally connected in the rodent model (Majeed et al., 2009; Williams et al., 2010), a single functional network may be over-represented in this "global" signal rather than a true whole-brain average. If this is the case, then regressing the global signal may be reducing the spatial extent of correlations within this network, rather than removing some large-scale physiological effect. Further work with sliding window correlation in human subject fMRI would help address these limits of the anesthetized rat model.

Because dynamic analysis of functional connectivity is a relatively new area (Chang and Glover, 2010; Majeed et al., 2009), it is still unclear how best to relate these dynamic changes to the global signal. In particular, testing multiple start locations within each window to compare to the global signal may not have been the best choice. Future work investigating the various sources that contribute to the global signal (neuronal and non-neuronal), and the ultimate origins of the dynamic changes in functional connectivity, may elucidate better ways to address this question than were presented in this study.

4.5. Limitations and future directions

Because anesthesia has a profound impact on both neural activity and the vasculature, it is important that these studies be extended to other anesthetic agents and, if possible, to awake rodents. However, it is likely that the findings will be similar; in awake nonhuman primates the fMRI signal was strongly related to beta and gamma field potentials (Goense and Logothetis, 2008) and exhibited correlation structures similar to BOLD in human pre-surgical patients (He et al., 2008).

Large errors were measured when attempting to determine the time shift of maximum correlation between BOLD and BLP sliding window series. Therefore, this study simply used the four second shift that was observed in previous, steady-state results (Pan et al., 2011, Figure 5). However, future work should investigate whether a "hemodynamic response function" truly exists when considering dynamic instead of steady state correlations.

Future studies should also examine other pairs of areas. Previous work has shown that the variability in BOLD correlation observed with sliding window techniques for left and right SI is quite different from the variability observed in randomly matched signals (Keilholz et al., 2012). However, other pairs of areas (SI and motor cortex) also exhibit some differences from the random distribution, and even areas where the distribution is statistically similar to randomly-matched data may actually contain information about neural activity. Simultaneous imaging and recording provides one way to link variability in the BOLD signal to an external measure of neural activity and verify that variability does not arise solely from inherent properties of the filtered, processed signal.

The finding that BLP exhibits variability in interhemispheric correlation that is closely linked to changes in BOLD correlation provides a firm basis for future explorations of network dynamics in the brain. For example, the prevalence and pattern of brain states can be examined, as has been done in several fMRI studies (Allen et al., 2012; Keilholz et al.,

2012; Liu and Duyn, 2013). Utilizing simultaneously acquired BLPs as an independent measure of neural activity can help in identifying whether rare, transient states have a neural basis.

4.6. Conclusions

As interest in dynamic changes in the fMRI signal increases, it becomes important to understand the neural-electrical dynamics that underlie the fMRI dynamics. While studies differentiating based on behavior or disease can suggest that fMRI dynamics are important, and EEG studies can suggest a neural basis, studies such as the present one are required to better understand this basis. This study showed that BOLD sliding window correlation in the anesthetized rat was significantly related to sliding window correlation calculated for simultaneously-recorded BLP, particularly for the theta, beta and gamma frequencies. These data show that at least part of the variability in the BOLD sliding window series is related to changes in neural activity.

Supplementary Material

Refer to Web version on PubMed Central for supplementary material.

Acknowledgments

Funding was provided by the National Institute of Health, 1R21NS072810-01A1 and 1R21NS057718-01, and the Scholarly Inquiry and Research at Emory graduate fellowship. The authors would like to acknowledge Alessio Medda, Martha Willis, Jacob Billings, Sadia Shakil and Rui Tang for their helpful comments, Jeremy Edgerton and Collin Lobb for their assistance with rodent electrophysiology, and Wendy Hu for proofreading. The authors would also like to thank the anonymous reviewers for their helpful comments, which resulted in the addition of Tables I and IV, Figure 5 and Supplemental Figures S1 through S4.

Abbreviations

fMRI	functional magnetic resonance imaging
BOLD	blood oxygen level dependent
LFP	local field potentials
EEG	electroencephalography
BLP	band-limited power
FFT	fast fourier transform
FIR	finite impulse response
SI	primary somatosensory cortex
SGoF	sequential goodness of fit
FWER	family-wise error rate

References

Alkire MT, Haier RJ, Fallon JH. Toward a unified theory of narcosis: brain imaging evidence for a thalamocortical switch as the neurophysiologic basis of anesthetic-induced unconsciousness. Conscious Cogn. 2000; 9:370–386. [PubMed: 10993665]

Allen EA, Damaraju E, Plis SM, Erhardt EB, Eichele T, Calhoun VD. Tracking Whole-Brain Connectivity Dynamics in the Resting State. Cereb Cortex. 2012

Allen PJ, Josephs O, Turner R. A method for removing imaging artifact from continuous EEG recorded during functional MRI. Neuroimage. 2000; 12:230–239. [PubMed: 10913328]

Biswal B, Yetkin FZ, Haughton VM, Hyde JS. Functional connectivity in the motor cortex of resting human brain using echo-planar MRI. Magn Reson Med. 1995; 34:537–541. [PubMed: 8524021]

Canolty RT, Knight RT. The functional role of cross-frequency coupling. Trends Cogn Sci. 2010; 14:506–515. [PubMed: 20932795]

Carvajal-Rodriguez A, de Una-Alvarez J, Rolan-Alvarez E. A new multitest correction (SGoF) that increases its statistical power when increasing the number of tests. BMC Bioinformatics. 2009; 10:209. [PubMed: 19586526]

Cason BA, Shubayev I, Hickey RF. Blockade of adenosine triphosphate-sensitive potassium channels eliminates isoflurane-induced coronary artery vasodilation. Anesthesiology. 1994; 81:1245–1255. discussion 1227A–1228A. [PubMed: 7978484]

Chang C, Glover GH. Time-frequency dynamics of resting-state brain connectivity measured with fMRI. Neuroimage. 2010; 50:81–98. [PubMed: 20006716]

Chang C, Liu Z, Chen MC, Liu X, Duyn JH. EEG correlates of time-varying BOLD functional connectivity. Neuroimage. 2013; 72:227–236. [PubMed: 23376790]

Cordes D, Haughton VM, Arfanakis K, Wendt GJ, Turski PA, Moritz CH, Quigley MA, Meyerand ME. Mapping functionally related regions of brain with functional connectivity MR imaging. AJNR Am J Neuroradiol. 2000; 21:1636–1644. [PubMed: 11039342]

Fox MD, Snyder AZ, Vincent JL, Corbetta M, Van Essen DC, Raichle ME. The human brain is intrinsically organized into dynamic, anticorrelated functional networks. Proc Natl Acad Sci U S A. 2005; 102:9673–9678. [PubMed: 15976020]

Fox MD, Zhang DY, Snyder AZ, Raichle ME. The Global Signal and Observed Anticorrelated Resting State Brain Networks. Journal of Neurophysiology. 2009; 101:3270–3283. [PubMed: 19339462]

Gavrilescu M, Shaw ME, Stuart GW, Eckersley P, Svalbe ID, Egan GF. Simulation of the effects of global normalization procedures in functional MRI. Neuroimage. 2002; 17:532–542. [PubMed: 12377132]

Goense JB, Logothetis NK. Neurophysiology of the BOLD fMRI signal in awake monkeys. Curr Biol. 2008; 18:631–640. [PubMed: 18439825]

Greicius MD, Srivastava G, Reiss AL, Menon V. Default-mode network activity distinguishes Alzheimer's disease from healthy aging: evidence from functional MRI. Proc Natl Acad Sci U S A. 2004; 101:4637–4642. [PubMed: 15070770]

Grigg O, Grady CL. Task-related effects on the temporal and spatial dynamics of resting-state functional connectivity in the default network. PLoS One. 2010; 5:e13311. [PubMed: 20967203]

Gruetter R. Automatic, localized in vivo adjustment of all first- and second-order shim coils. Magn Reson Med. 1993; 29:804–811. [PubMed: 8350724]

Handwerker DA, Roopchansingh V, Gonzalez-Castillo J, Bandettini PA. Periodic changes in fMRI connectivity. Neuroimage. 2012; 63:1712–1719. [PubMed: 22796990]

He BJ, Snyder AZ, Zempel JM, Smyth MD, Raichle ME. Electrophysiological correlates of the brain's intrinsic large-scale functional architecture. Proc Natl Acad Sci U S A. 2008; 105:16039–16044. [PubMed: 18843113]

Honey CJ, Kotter R, Breakspear M, Sporns O. Network structure of cerebral cortex shapes functional connectivity on multiple time scales. Proc Natl Acad Sci U S A. 2007; 104:10240–10245. [PubMed: 17548818]

Hutchison RM, Womelsdorf T, Allen EA, Bandettini PA, Calhoun VD, Corbetta M, Della Penna S, Duyn J, Glover G, Gonzalez-Castillo J, Handwerker DA, Keilholz S, Kiviniemi V, Leopold DA, de Pasquale F, Sporns O, Walter M, Chang C. Dynamic functional connectivity: Promises, issues, and interpretations. Neuroimage. 2013

Hutchison RM, Womelsdorf T, Gati JS, Everling S, Menon RS. Resting-state networks show dynamic functional connectivity in awake humans and anesthetized macaques. Hum Brain Mapp. 2012

Keilholz S, Magnuson ME, Pan WJ, Willis M, Thompson G. Dynamic Properties of Functional Connectivity in the Rodent. Brain Connect. 2012

Kiviniemi V, Vire T, Remes J, Elseoud AA, Starck T, Tervonen O, Nikkinen J. A sliding time-window ICA reveals spatial variability of the default mode network in time. Brain Connect. 2011; 1:339–347. [PubMed: 22432423]

Liu X, Duyn JH. Time-varying functional network information extracted from brief instances of spontaneous brain activity. Proc Natl Acad Sci U S A. 2013; 110:4392–4397. [PubMed: 23440216]

Liu X, Zhu XH, Zhang Y, Chen W. Neural Origin of Spontaneous Hemodynamic Fluctuations in Rats under Burst-Suppression Anesthesia Condition. Cereb Cortex. 2010; 21:374–384. [PubMed: 20530220]

Liu X, Zhu XH, Zhang Y, Chen W. The Change of Functional Connectivity Specificity in Rats Under Various Anesthesia Levels and its Neural Origin. Brain Topogr. 2012

Lowe MJ, Dzemidzic M, Lurito JT, Mathews VP, Phillips MD. Correlations in low-frequency BOLD fluctuations reflect cortico-cortical connections. Neuroimage. 2000; 12:582–587. [PubMed: 11034865]

Magnuson M, Majeed W, Keilholz SD. Functional connectivity in blood oxygenation level-dependent and cerebral blood volume-weighted resting state functional magnetic resonance imaging in the rat brain. J Magn Reson Imaging. 2010; 32:584–592. [PubMed: 20815055]

Magri C, Schridde U, Murayama Y, Panzeri S, Logothetis NK. The amplitude and timing of the BOLD signal reflects the relationship between local field potential power at different frequencies. J Neurosci. 2012; 32:1395–1407. [PubMed: 22279224]

Majeed W, Magnuson M, Hasenkamp W, Schwarb H, Schumacher EH, Barsalou L, Keilholz SD. Spatiotemporal dynamics of low frequency BOLD fluctuations in rats and humans. Neuroimage. 2011; 54:1140–1150. [PubMed: 20728554]

Majeed W, Magnuson M, Keilholz SD. Spatiotemporal dynamics of low frequency fluctuations in BOLD fMRI of the rat. J Magn Reson Imaging. 2009; 30:384–393. [PubMed: 19629982]

Monto S, Palva S, Voipio J, Palva JM. Very slow EEG fluctuations predict the dynamics of stimulus detection and oscillation amplitudes in humans. J Neurosci. 2008; 28:8268–8272. [PubMed: 18701689]

Pan WJ, Thompson G, Magnuson M, Majeed W, Jaeger D, Keilholz S. Simultaneous FMRI and electrophysiology in the rodent brain. J Vis Exp. 2010

Pan WJ, Thompson G, Magnuson M, Majeed W, Jaeger D, Keilholz S. Broadband local field potentials correlate with spontaneous fluctuations in functional magnetic resonance imaging signals in the rat somatosensory cortex under isoflurane anesthesia. Brain Connect. 2011; 1:119–131. [PubMed: 22433008]

Pan WJ, Thompson GJ, Magnuson ME, Jaeger D, Keilholz S. Infraslow LFP correlates to resting-state fMRI BOLD signals. Neuroimage. 2013; 74C:288–297. [PubMed: 23481462]

Paxinos, G.; Watson, C. The rat brain in stereotaxic coordinates. 5. Elsevier Academic Press; Amsterdam; Boston: 2005.

Raichle ME, MacLeod AM, Snyder AZ, Powers WJ, Gusnard DA, Shulman GL. A default mode of brain function. Proc Natl Acad Sci U S A. 2001; 98:676–682. [PubMed: 11209064]

Reiz S, Balfors E, Sorensen MB, Ariola S Jr, Friedman A, Truedsson H. Isoflurane--a powerful coronary vasodilator in patients with coronary artery disease. Anesthesiology. 1983; 59:91–97. [PubMed: 6869900]

Rombouts SA, Barkhof F, Goekoop R, Stam CJ, Scheltens P. Altered resting state networks in mild cognitive impairment and mild Alzheimer's disease: an fMRI study. Hum Brain Mapp. 2005; 26:231–239. [PubMed: 15954139]

Sakoglu U, Pearlson GD, Kiehl KA, Wang YM, Michael AM, Calhoun VD. A method for evaluating dynamic functional network connectivity and task-modulation: application to schizophrenia. Magma. 2010; 23:351–366. [PubMed: 20162320]

Scholvinck ML, Maier A, Ye FQ, Duyn JH, Leopold DA. Neural basis of global resting-state fMRI activity. Proc Natl Acad Sci U S A. 2010; 107:10238–10243. [PubMed: 20439733]

Shmuel A, Leopold DA. Neuronal correlates of spontaneous fluctuations in fMRI signals in monkey visual cortex: Implications for functional connectivity at rest. Hum Brain Mapp. 2008; 29:751–761. [PubMed: 18465799]

Tagliazucchi E, von Wegner F, Morzelewski A, Brodbeck V, Laufs H. Dynamic BOLD functional connectivity in humans and its electrophysiological correlates. Front Hum Neurosci. 2012; 6:339. [PubMed: 23293596]

Thompson GJ, Magnuson ME, Merritt MD, Schwarb H, Pan WJ, McKinley A, Tripp LD, Schumacher EH, Keilholz SD. Short-time windows of correlation between large-scale functional brain networks predict vigilance intraindividually and interindividually. Hum Brain Mapp. 2012

Tian L, Jiang T, Wang Y, Zang Y, He Y, Liang M, Sui M, Cao Q, Hu S, Peng M, Zhuo Y. Altered resting-state functional connectivity patterns of anterior cingulate cortex in adolescents with attention deficit hyperactivity disorder. Neurosci Lett. 2006; 400:39–43. [PubMed: 16510242]

Tort AB, Komorowski R, Eichenbaum H, Kopell N. Measuring phase-amplitude coupling between neuronal oscillations of different frequencies. J Neurophysiol. 2010; 104:1195–1210. [PubMed: 20463205]

van de Ven VG, Formisano E, Prvulovic D, Roeder CH, Linden DE. Functional connectivity as revealed by spatial independent component analysis of fMRI measurements during rest. Hum Brain Mapp. 2004; 22:165–178. [PubMed: 15195284]

Villalobos ME, Mizuno A, Dahl BC, Kemmotsu N, Muller RA. Reduced functional connectivity between V1 and inferior frontal cortex associated with visuomotor performance in autism. Neuroimage. 2005; 25:916–925. [PubMed: 15808991]

Williams KA, Magnuson M, Majeed W, LaConte SM, Peltier SJ, Hu X, Keilholz SD. Comparison of alpha-chloralose, medetomidine and isoflurane anesthesia for functional connectivity mapping in the rat. Magn Reson Imaging. 2010; 28:995–1003. [PubMed: 20456892]

Highlights

- fMRI and electrophysiology data were recorded simultaneously from rats.
- Time-windowed correlation between bilateral somatosensory cortex was examined.
- fMRI connectivity variations matched electrophysiology connectivity variations.
- Bilateral correlation plateaued at a short window length, approximately 50 seconds.
- Electrophysiology-fMRI correlation and error increased with window length.

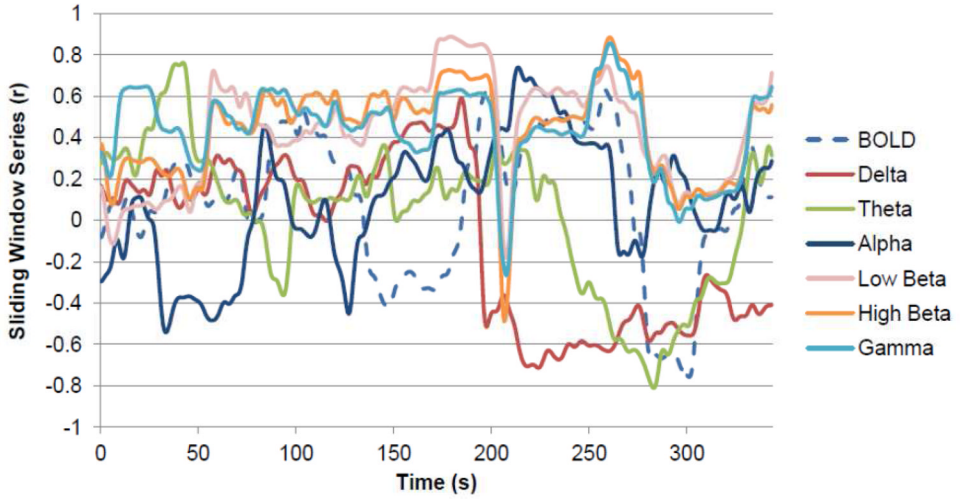

Figure 1.

Example of interhemispheric correlation, measured in a sliding window as a function of window start time ("sliding window series") from one rat, one fMRI run. Values are calculated using a window length of 50s, between left and right SI, for BOLD (dashed line) and each BLP band (solid lines, colors shown in legend), and are plotted versus the time of each window's start point. Correlation varies substantially over time for all signals, ranging from strongly positive to strongly negative for BOLD, delta, theta, and alpha. Beta and gamma band correlation is rarely negative in this example, yet still varies between zero and high positive values.

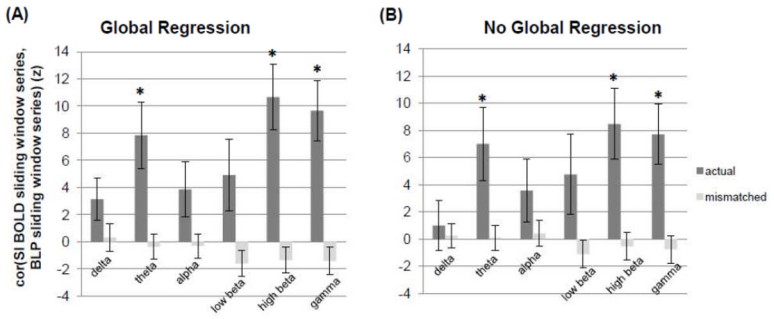

Figure 2.

(A) Mean correlation (normalized z values) between SI BOLD sliding window series and BLP sliding window series for each frequency band, after global signal regression. Correlation between the SI BOLD sliding window series and the BLP time courses for signals from incorrectly matched runs are shown as a control. Error bars are one standard error. The highest correlation is observed in high beta and gamma bands. Theta, high beta and gamma bands exhibited significant correlation to the SI BOLD sliding window series after correction for multiple comparisons when compared to randomly matched SI BOLD and BLP pairs (t-test, p values: delta 0.272, theta 1.35×10^{-3}, alpha 7.65×10^{-2}, low beta 1.45×10^{-2}, high beta 8.40×10^{-6}, gamma 5.18×10^{-5}). **(B)** The same calculations were performed for data without global signal regression. All values are slightly lower, but the same three bands remain significance (t test, p values: delta 0.743, theta 7.20×10^{-3}, alpha 0.214, low beta 3.59×10^{-2}, high beta 1.35×10^{-3}, gamma 1.81×10^{-3}). Error bars are one standard error. This figure was calculated with a 50s long sliding window and with BLP lagged four seconds after SI BOLD.

* Statistically significant at 5% passing multiple comparisons correction (Carvajal-Rodriguez et al., 2009).

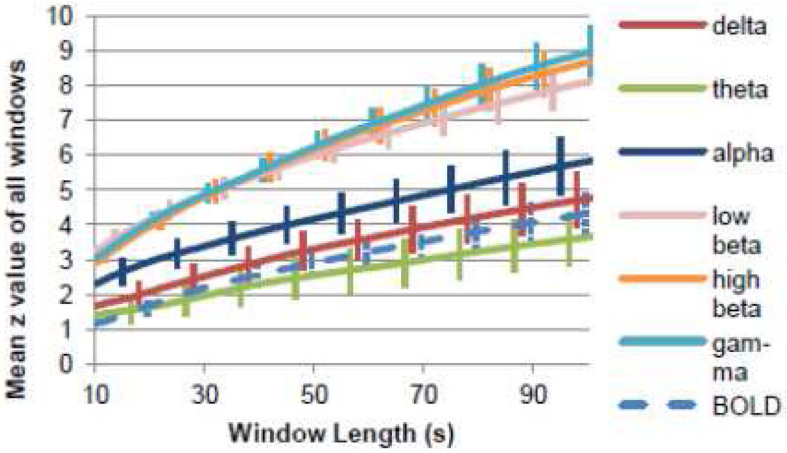

Figure 3.

Mean of normalized z values for interhemispheric SI correlation, over all windows and all runs, for BOLD and each BLP band, plotted versus window length. Error bars are one standard error in terms of inter-trial variance. For visibility purposes, only every 20th error bar is shown, and they are staggered between plots. As they were calculated from two second long segments, theta and delta include information from up to 1.5s longer than the window length used for correlation. Positive correlation is present for all bands even at the shortest windows, and increases steadily as window length increases. This plot uses normalized z scores, for naïve correlations see Supplemental figure S1.

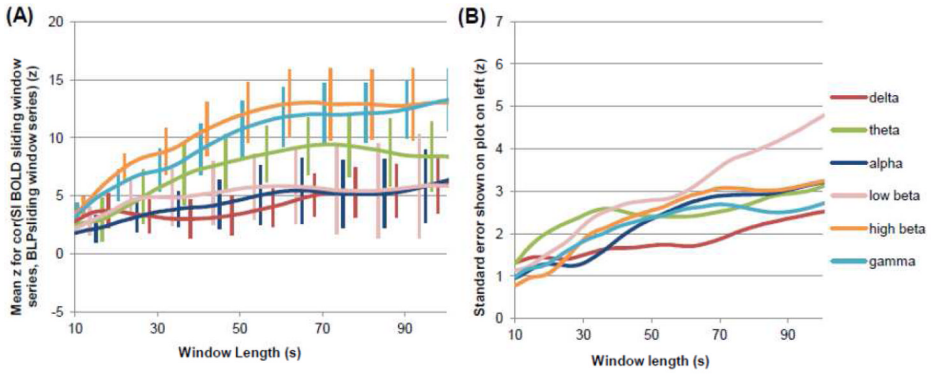

Figure 4.

(A) Mean of normalized z values for correlation between BOLD sliding window series and each BLP sliding window series (shifted 4s prior), over all runs, plotted versus window length. Error bars are one standard error in terms of inter-trial variance. For visibility purposes, only every 20th error bar is shown, and they are staggered between plots. As they were calculated from two second long segments, theta and delta may include information from up to 1.5s longer than the window length used for correlation. (B) Standard error of z values plotted in (A), these are the same values shown on the error. Note that correlation steadily increases until it reaches a plateau, and error appears to steadily increase with window length. This plot uses normalized z scores, for naïve correlations, see Supplemental figure S2.

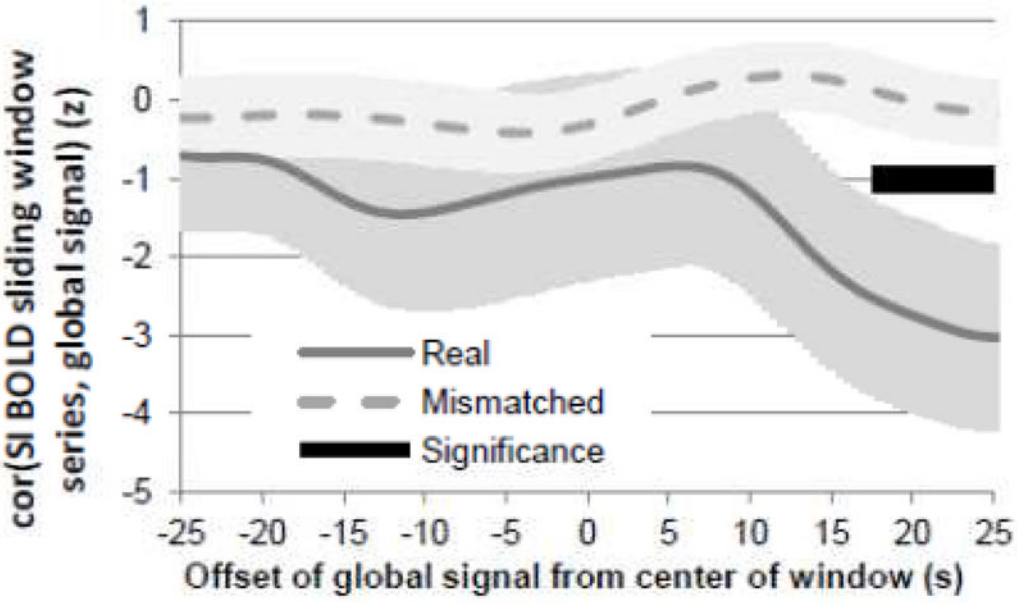

Figure 5.

Correlation between the sliding window series from SI BOLD where no global regression has been performed versus the "global signal," i.e. the mean BOLD signal from the whole brain. Ordinate is the normalized z value calculated from the correlation, abscissa is the relative time point within the window (used to calculate the sliding window series) where the corresponding point from the global signal was taken; negative numbers indicate earlier points in the window, positive numbers indicate later points. The darker gray solid line is from correctly matched SI BOLD sliding window series with global signals, the lighter gray dashed line is from incorrect matching. The lighter colored borders around each line represent one standard error. The two lines are significantly different at alignments from 17.5s to 25s ($0.0210 \leq p \leq 0.0125$, threshold of $p=0.05$ corrected for multiple comparisons with SGoF), this is shown with a black bar. The negative correlation values suggest that increases in global signal decrease amplitude of sliding window correlation, and/or vice-versa. Note that, while theoretically possible (see section 2.12), no statistical significance was seen if global regression was performed on SI BOLD prior to the calculation of the sliding window series (see section 3.4 and Supplemental Figure S4).

Table I

Isoflurane levels, number of runs used and date recorded from each rat.

Rat index	Date	Number of runs	Isoflurane levels (%)
1*	11/6/2009	2	1.5
2	11/7/2009	1	1.3
3	11/12/2009	1	1.5
		1	1.4
4	11/13 /2009	1	1.8
5	11/14/2009	3	1.5
6	11/20/2009	1	1.5
		1	1.2–2.0**
7	11/21 /2009	2	1.5
Total		**13**	**1.2–2.0**

* The first run from this rat is plotted in figure one.

** Anomalous breathing was noticed approximately halfway through the run and isoflurane was increased to 2% to follow our protocol.

Table II

Mean interhemispheric correlation (normalized z values) between left and right SI signals for BOLD and each BLP signal. Estimated Pearson correlation (*r*) values are also shown; these were created by applying the inverse transformation to the z values shown in the column to the left. Compare *r* values to figure 7 of Pan, et al. (Pan et al., 2011).

	Mean Bilateral Steady State Correlation	
	Normalized z	**Estimated r**
BOLD	8.5 ± 4.3	0.293 ± 0.151
Delta	9.0 ± 4.9	0.309 ± 0.174
Theta	7.4 ± 5.2	0.258 ± 0.182
Alpha	12.1 ± 7.1	0.406 ± 0.247
Low Beta	16.4 ± 4.4	0.525 ± 0.153
High Beta	16.5 ± 5.1	0.527 ± 0.179
Gamma	16.4 ± 5.2	0.525 ± 0.184

Mean ± one standard error is shown for each signal.

Table III

Mean correlations for interhemispheric SI sliding correlation for BOLD and every BLP frequency band. Results are shown for the shortest window length (10s), the window length used in most tests in this study (50 seconds), and the longest window length (100 seconds).

	10s	50s	100s	10s (naïve)	50s (naïve)	100s (naïve)
BOLD	1.17 ± 0.06	2.91 ± 0.11	4.33 ± 0.17	0.16 ± 0.01	0.25 ± 0.01	0.28 ± 0.01
Delta	1.67 ± 0.10	3.31 ± 0.16	4.75 ± 0.22	0.21 ± 0.01	0.28 ± 0.01	0.30 ± 0.01
Theta	1.40 ± 0.10	2.55 ± 0.17	3.65 ± 0.22	0.18 ± 0.01	0.22 ± 0.01	0.24 ± 0.01
Alpha	2.29 ± 0.09	4.17 ± 0.15	5.83 ± 0.23	0.29 ± 0.01	0.34 ± 0.01	0.36 ± 0.01
Low beta	3.25 ± 0.07	5.98 ± 0.11	8.11 ± 0.18	0.40 ± 0.01	0.48 ± 0.01	0.49 ± 0.01
High beta	2.90 ± 0.06	6.16 ± 0.12	8.66 ± 0.20	0.37 ± 0.01	0.48 ± 0.01	0.50 ± 0.01
Gamma	3.03 ± 0.06	6.24 ± 0.11	8.95 ± 0.20	0.38 ± 0.01	0.48 ± 0.01	0.51 ± 0.01

Mean ± one standard error is shown. The first three columns are normalized z values, the last three columns are naïve *r* values. As they were calculated from two second long segments, theta and delta may include information from up to 1.5s longer than the window length used for correlation. Note that normalized z values increase greatly with window length, but naïve *r* values plateau around the 50s window length. Also note that errors are comparatively small in most cases.

Table IV

SI BOLD, BLP and global BOLD signals in partial correlation analysis. Partial correlation was performed for three signals, the BOLD signal from SI, a BLP signal and the global BOLD signal (each column is partial correlation between two signals). This was repeated for every BLP band in this study (each row is a frequency band).

	SI-BOLD vs. BLP z	SI-BOLD vs. Global z	BLP vs. Global z
Delta	5.51 ± 0.21	*15.54 ± 0.24	−2.05 ± 0.13
Theta	*7.07 ± 0.17	*14.61 ± 0.24	−0.07 ± 0.11
Alpha	7.26 ± 0.18	*14.51 ± 0.23	0.22 ± 0.13
Low beta	*8.95 ± 0.13	*14.12 ± 0.23	0.40 ± 0.14
High beta	*9.55 ± 0.11	*14.45 ± 0.24	−0.59 ± 0.14
Gamma	*8.93 ± 0.12	*14.54 ± 0.24	−0.61 ± 0.12

Values shown are normalized z scores calculated from partial correlation values for the corresponding row/column, mean ± one standard error. The significance threshold used here was 0.05 corrected for multiple comparisons with SGoF ($p \leq 1.70\times10^{-31}$). For SI BOLD vs. BLP, theta, beta and gamma were statistically significant (p values: $5.94\times10^{-17} \geq p \geq 2.24\times10^{-31}$ for non-significant, $1.70\times10^{-31} \geq p \geq 1.12\times10^{-48}$ for significant, effect size: $7.70 \geq \Delta z \geq 5.78$ for non-significant, $9.73 \geq \Delta z \geq 7.35$ for significant). For SI BOLD vs. global BOLD all results were statistically significant ($2.81\times10^{-67} \geq p \geq 4.82\times10^{-78}$, effect size: $15.6 \geq \Delta z \geq 14.1$). For BLP vs. global BOLD no results were statistically significant ($0.766 \geq p \geq 8.66\times10^{-4}$, effect size: $2.24 \geq \Delta z \geq 0.163$). The reason alpha is not statistically significant despite having a slightly higher z score (and effect size) than theta is because it had slightly higher errors in both correctly and incorrectly matched data.

*Statistically significant at 5% passing multiple comparisons correction (Carvajal-Rodriguez et al., 2009).